Journal of Food Engineering 335 (2022) 111190

Contents lists available at ScienceDirect

Journal of Food Engineering

journal homepage: www.elsevier.com/locate/jfoodeng

Active caseinate/guar gum films incorporated with gallic acid: Physicochemical properties and release kinetics

Muhammad Rehan Khan [a], Stefania Volpe [a], Emiliano Salucci [a], Muhammad Bilal Sadiq [b], Elena Torrieri [a,*]

[a] Department of Agricultural Science, University of Naples Federico II, Via Università 133, 80055, Portici, NA, Italy
[b] School of Life Sciences, Forman Christian College (A Chartered University), Lahore, Pakistan

ARTICLE INFO

Keywords:
Sodium caseinate
Guar gum
Gallic acid
Active packaging
Release kinetics
Molecular modelling

ABSTRACT

Composite active films based on sodium caseinate/guar gum were prepared by the incorporation of gallic acid at different concentrations to investigate its effect on the structure, physicochemical properties, and the release kinetics from the film. The incorporation of gallic acid imparted changes in the FT-IR spectra. Water vapor permeability (WVP) of films decreased up to 21% after the incorporation of gallic acid in the film. The gallic acid released from the films GAI$^{*60\ \mu g.ml^{-1}}$, GAII$^{*250\ \mu g.ml^{-1}}$ and GAIII$^{*650\ \mu g.ml^{-1}}$ was 67%, 32% and 30% respectively. Similarly, the diffusion coefficient was also affected by an increase in the concentration and was: $8.10 \times 10^{-12}\ m^2s^{-1}$, $6.23 \times 10^{-12}\ m^2s^{-1}$, and $4.5 \times 10^{-12}\ m^2s^{-1}$ for GAI, GAII and GAIII films respectively. Molecular docking suggested the potential inactivation of oxidative enzymes due to binding of gallic acid near their active sites. Therefore, gallic acid releasing films maybe considered as an active food packaging for fruits and vegetables (F&V).

1. Introduction

Active antioxidant films have shown promising results in preserving the nutritional quality of minimally processed F&V (Khan et al., 2021a, b). The addition of synthetic active additives i.e., amines, alcohols, organic and in-organic acids into plastic-based materials has led to environmental and public health concerns. Due to the non-biodegradable nature and disposal problems of plastics, the screening of natural biodegradable alternatives is at the rise in the past decade (Asgher et al., 2020).

Biopolymers derived from agro-livestock resources can provide an effective solution to this problem. Usually, protein-based films present good mechanical and barrier properties (against gases) as compared to other biopolymeric materials. For instance, casein is a milk protein having excellent tendency for degradation, emulsification, carrier of bioactive compounds, and high thermal stability, which makes it a highly desirable macromolecule to produce packaging films (Khan et al., 2021a,b). Guar gum has been used as a thickener and reinforcing agent for caseinate based film (Alizadeh-Sani et al., 2020), to improve its mechanical properties. However, the hydrophilic nature of caseinate restricts its application in food packaging. Several strategies have been employed to counter this problem i.e., blending with other biopolymers and incorporating food additives. Nevertheless, the possibility of cross-linking phenolic compounds can provide solution to this problem since certain polyphenolic compounds can improve physicochemical properties by modifying the structure of the polymeric matrices upon interaction and their release into the food metrices can be modulated which can have a significant influence not only on the shelf-life of the product but also on the improvement of public health (LakshmiBalasubramaniam et al., 2022).

Recently, tea waste extracts extracted by formic acid displayed high yield of epigallocatechin gallate which is an ester of gallic acid and epigallocatechin-3-gallate and exhibited an IC_{50} value of 73.1 μg/ml (Quilez-Molina et al., 2020). Gallic Acid (3,4,5-trihydroxybenzoic acid) is a naturally occurring low-molecular weight triphenolic acid which is found in green tea, vegetables, and fruits with a wide range of biological activities i.e., antimicrobial, antioxidant and anticancer (Tapia--Hernández et al., 2019). Furthermore, gallic acid has been utilized for the development of food packaging with certain polymeric materials (i.e., chitosan) because of its acidic pH and solubility issues (Yadav et al., 2021; Rui et al., 2017). However, these issues can be resolved by mixing the biopolymer and the gallic acid in a buffer. Furthermore, limited

* Corresponding author. Via Universitá 100, Parco Gussone, Edifico H, 80055, Portici, NA, Italy.
E-mail address: elena.torrieri@unina.it (E. Torrieri).

https://doi.org/10.1016/j.jfoodeng.2022.111190
Received 4 April 2022; Received in revised form 13 June 2022; Accepted 17 June 2022
Available online 22 June 2022

literature in available on the development of active packaging forms by utilizing casein-based economical biodegradable alternatives with gallic acid.

To properly develop an active packaging, it is essential to consider the interactions between packaging components to bring advancements in packaging domain (Khan et al., 2021a,b; Volpe et al., 2017). Since knowledge of these interactions could elucidate the release behavior of gallic acid from the packaging material into the food metrices. The diffusion coefficients (D) estimated by using mathematical models based on Fick's Second Law can provide essential information on modulating this release behavior of bioactive from the package to ensure compliance with regulatory measures set by Food Safety Authorities for designing novel packaging. Furthermore, importance of release kinetic parameters (i.e., partition coefficient and diffusivity) of a bioactive compound from a packaging film should also be considered since it has a role in controlling the shelf life of the product (Benbettaieb et al., 2021). In a previous work, molecular docking was used to elucidate interactions between phenolic acids and casein fractions and results showed that gallic acid had good binding ability with α-casein subunits due to their hydrophilicity. The diffusion coefficient of gallic acid in casein film were estimated at 5.99 × 10–12 m^2/s (Khan et al., 2022). Although several studies have been conducted to elucidate the release of bioactive compound from the packaging materials into different matrices (Benbettaïeb et al., 2020; Dede et al., 2022; Requena et al., 2017), still to the best of our knowledge, the approach to elucidate the influence of gallic acid on its release from caseinate/guar film with mathematical modelling has never been carried out.

Previously, the research was focused to design packaging materials to restrict lipid oxidation in food products from animal origin (Domínguez et al., 2018), whereas loss of nutritional quality in minimally processed fruits and vegetables (F&V) due to oxidation reactions has not been given much attention. One of the reasons of oxidation of essential nutrients is the activation of oxidizing enzymes i.e., polyphenol oxidase (PPO), ascorbate oxidase (AO) due to various factors (Khan et al., 2021a, b). Several studies have been employed for the inactivation of oxidative enzymes i.e., by using light (i.e., pulsed) and temperature (i.e., conventional heating and microwave) (Cavalcante et al., 2021; Manzocco et al., 2013); however, inactivation of oxidizing enzymes by using phenolic compounds is still a new concept especially in food packaging domain.

Thus, the objective of this study was to investigate the influence of gallic acid on the film structure, to quantify its antioxidant properties and to describe the release mechanism by mathematical modelling.

2. Materials and methods

2.1. Materials

Gallic acid (91215), sodium caseinate from bovine milk (C8654), glycerol (ACS reagent, ≥ 99.5%), DPPH (2,2-Diphenyl-1-(2,4,6-trinitrophenyl) hydrazyl) D9132, ABTS (2,2`-Azino-bis-(3-ethylbenzothiazoline sulfonate-6-sulfonic acid), ethanol (96%) were acquired from Sigma-Aldrich (Milan, Italy). Guar gum was acquired from Sigma-Aldrich, Pakistan. All other reagents used were of analytical grade.

2.2. Film formulation

Film samples were prepared by using solution casting method given by (Alizadeh-Sani et al., 2020) with modifications. Briefly, gallic acid (Sigma-Aldrich, Milan, Italy) in three different concentrations (based on initial trial in which an IC_{50} of ~30 μg/ml against DPPH assay was reported for gallic acid and mentioned elsewhere, thus, 60 μg $ml^{-1}{}_{*GAI}$, 250 μg.$ml_{.1*GAII}$, and 650 μg $ml^{-1}{}_{*GAIII}$ of the film forming solution (FFS) were selected to achieve ≥80% inhibition against DPPH) was dissolved separately in 20 ml freshly prepared 0.02 M Tris buffer (pH 8) under continuous magnetic stirring for 30 min at room temperature (Khan et al., 2022). On the other hand, 8 g of sodium caseinate (Sigma-Aldrich, Milan, Italy), guar gum (0.2 g) (Sigma-Aldrich, Pakistan), and glycerol (10% w/w of the total solid content) were dissolved in 0.02 M Tris buffer (80 ml: pH 8) for 3 h under stirring at 70 ± 2 °C. After a homogenous mixture was obtained, the FFS was cooled down at room temperature, and gallic acid solutions were incorporated, followed by stirring to obtain a final solution. For control films without gallic acid (casein and casein/guar gum) similar procedure was followed. Final FFS (5 ml) was then casted onto the petri dishes (56.7 cm^2 surface area) and dried at 30 °C and 57 ± 2% relative humidity overnight in the climatic chamber (MMM Medcenter Einrichtungen, Germany).

2.3. Physical characterization

2.3.1. Film thickness

The thickness of the film samples was measured by using a digital hand-held micrometer (H062, Metacontrol, Napoli, Italy) with a sensitivity of 0.002 mm. The average film thickness was estimated by taking measurements at eight different locations.

2.3.2. Water vapor permeability

The water vapor permeability (WVP) of the film samples was evaluated gravimetrically according to ASTM through Payne permeability cups (Carlo Erba, Milan, Italy) as reported by Volpe et al., (2017). Briefly, 8 g of silica gel was added into each cup, and a film surface of 9.89 cm^2 was exposed to vapor transmission. All the cups were then placed inside a desiccator containing saturated KCl solution (85% RH). The cups were weighed regularly and water vapor transmission rate through film samples was estimated by linear portion of diagram by plotting an increment in cup weight as a function of time. The WVP was calculated at 20 °C by following equation:

$$WVP = \frac{WVTR.x}{\Delta_P} \quad (1)$$

where WVTR is the water vapor transmission rate (g m^{-2} s^{-1}), x is the film thickness (m), and ΔP is the partial water vapor pressure difference between the two film sides (Pa).

2.3.3. Water solubility

Water solubility (WS) of the film samples was determined by the method given by Núñez-Flores et al. (2012) with modifications. Briefly, film samples (2 cm × 2 cm) were weighed and placed in falcon tubes (50 ml) containing 15 ml distilled water, overnight at 30 °C. The solution was then filtered through Whatmann filter paper No.1 to recover undissolved film sample, which was then placed in an oven at 105 °C for 24 h. Film solubility was calculated by following equation:

$$WS(\%) = \frac{w_i - w_f}{w_i} \times 100 \quad (2)$$

where Wi is the initial weight of the film samples and Wf is the final weight of the undissolved film residue.

2.3.4. Water contact angle (WCA)

A sessile drop method was used to determine the surface hydrophobicity of the caseinate films based on optical contact angle (°). Briefly, a 3 μl drop of ultrapure water was dropped on the film surface and the images were recorded for a period of 20 s at one image per second. The contact angle was calculated by using contact angle plugin of ImageJ software.

2.3.5. Mechanical properties

A universal testing machine (Instron, 5900R-4467, USA) was used to measure the mechanical properties of the samples according to the ASTM-D882-00 standard (Di Giuseppe et al., 2022). A load cell of 1 kN was used with a mechanical cross head speed of 50 mm/min. The

stress-strain curves obtained initially were used to determine tensile strength (TS), elongation at break (EAB), and elastic modulus (EM).

2.3.6. Color parameters

Color parameters of the film samples were evaluated by using Chromameter (Minolta, CR300, Osaka, Japan). The total color difference (ΔE) of the film samples was calculated by using Eq. (1) given by Yong et al. (2019):

$$\Delta E = \sqrt{(L^* - L)^2 + (a^* - a)^2 + (b^* - b)^2} \tag{3}$$

where, L, a and b indicates lightness, red-green, and yellow-blue coordinates of the color space CIELab respectively. Furthermore, a white standard plate (with L* = 96.94, a* = 0.23, and b* = 1.85) was used for calibration and on which samples were placed for measurement of color parameters.

The whiteness index (WI) was calculated by using the equation:

$$WI = 100 - \sqrt{(100 - L)^2 + (a)^2 + (b)^2} \tag{4}$$

2.3.7. UV-VIS spectroscopy and opacity

To determine the barrier properties of the films against visible and UV-light, dried film samples were directly placed in the test cell of a UV-VIS spectrophotometer (JASCO, V550, Tokyo, Japan) and percentage transmittance was measured from 300 to 700 nm at 25 ± 1 °C. On the other hand, air was used as a reference.

The absorbance of the film samples was measured at 660 nm and opacity was calculated by following equation:

$$Opacity = \frac{Abs_{660}}{x} \tag{5}$$

where Abs_{660} is the absorbance of the film samples at 660 nm and x is the thickness (mm) of the sample.

2.4. Release kinetics of gallic acid

The specific migration of gallic acid from caseinate based film samples was evaluated by using 95% ethanol solution only (since films disintegrated at lower ethanol concentrations) as food simulant according to European Commission Regulation (EU) No October 2011 and by following the protocol of Luzi et al. (2019) with slight modifications. All the film samples (10 cm^2) were totally immersed (double sided) into 20 ml of the food simulant (with area/volume ratio ~5 $dm^2\ L^{-1}$) at 30 °C in the incubator (Memmert, Model: 30–1060, Germany). Concentration of the active compounds in the simulant were determined by UV–Vis Spectroscopy (JASCO, V550, Tokyo, Japan) at 270 nm. The samples were taken out and evaluated at regular intervals (1, 3, 5, 24, 48, 72, 192 and 264 h) of time. Additionally, a blank test was also done for the simulant. To estimate the quantity of gallic acid released from the film into the simulant a standard calibration curve (1–25 μg ml^{-1}) was used. The results were expressed as μg.ml^{-1} of the simulant.

2.5. Mathematical modelling

Mathematical models are useful in describing physical mechanisms of release kinetics of an active compound from the polymeric chains into the food simulant by applying Fick's Second Law (Crank, 1979). The diffusion coefficient (D) of bioactive can be expressed by applying Fick's Law if we consider limited migration of gallic acid from limited film volume into limited volume of the food simulant. Thus, if we consider: a) unidimensional isothermal release of gallic acid from a thin film of thickness (e), b) uniform distribution of gallic acid in the food simulant at concentration M_∞, c) and at concentration M_t, the initial distribution of gallic acid in film matrix is homogenous (Rubilar et al., 2017). If diffusion occurs from both sides, the Fick's Law can be solved numerically by using finite differences methodology (solving the non-linear terms of partial differential equation also known as ordinary differential equations in which unknown variable is migrant concentration at each nodal point of the system). The Fick's second Law, boundary conditions and differential equation are as follows:

$$\frac{\partial C(x,t)}{\partial t} = D\left[\frac{\partial^2 C(x,t)}{\partial x^2}\right] \tag{6}$$

$$\begin{cases} \left.\dfrac{dC_i(t)}{d_t}\right|_{i=1} = 0 \\ \left.\dfrac{dC_i(t)}{dt}\right|_{i=n} = 0 \end{cases} \tag{7}$$

where C is the ratio between the concentration of the migrant at time (t) and its concentration after infinite time ($M_{f,\infty}$), D is the effective constant diffusivity.

In order to simplify the solution of the partial differential equation (PDE) of the second Fick's law, the method of lines on the second derivative with respect to the spatial variable was used. This approximation transforms the PDE into an ordinary differential equation (ODE) (equation (8)):

$$\frac{dC_i(t)}{dt} = D\frac{(C_{i-1}(t) - 2C_i(t) + C_{i+1}(t))}{x^2} \tag{8}$$

x is the distance from the interface obtained by dividing thickness of the material (e) divided by the total number of layers (n).

$$C = \frac{M_{f,t}}{M_{f,\infty}} \tag{9}$$

$$x = \frac{e}{n} \tag{10}$$

Root mean square error (RMSE) was calculated by using MATLAB to compare predicted and experimental models, to validate the mathematical models and to ensure the quality of fit (MATLAB, version 2021b, MathWorks, USA).

$$RMSE = \sqrt{\frac{\sum_{i=1}^{N}(\hat{y}_i - y_i)^2}{N}} \tag{11}$$

whereas, N is the total number of observations, while $\hat{y}_i$ and y_i are the residual values of observed and predicted values respectively.

Furthermore, partition coefficient (K) can be described as the ratio of the migrant in the food simulant ($C_{s,\infty}$) to the migrant in the polymeric matrix ($C_{F,\infty}$) once plateau is reached (Marvdashti et al., 2019).

$$K = \frac{C_{s,\infty}}{C_{F,\infty}} \tag{12}$$

2.6. Antioxidant activity

2.6.1. DPPH radical scavenging activity of the food simulant

The antioxidant activity of previously recovered food simulant solutions at each interval of time was estimated according to the protocol given by Luzi et al. (2019) with slight modifications. Initially, 1 ml of food simulant was mixed with 1.5 ml of DPPH solution (25 ppm) and incubated at room temperature for 30 min in the dark. The absorbance was recorded at 517 nm by using a spectrophotometer. The DPPH radical scavenging activity was calculated by using the following equation:

$$DPPH\ (\%) inhibition = \frac{AC - AS}{AC} \times 100 \tag{13}$$

where AC is the absorbance of control and AS is the absorbance of the sample.

2.6.2. ABTS radical scavenging activity of the films

The antioxidant potential of the film samples in terms of ABTS radical scavenging assay was evaluated by following protocol given by Hanani et al. (2019) with modifications. Briefly, freshly prepared ABTS solution (7 mM) was mixed with potassium persulfate solution (2.45 mM) with 1:1 vol ratio at 25 °C in the darkness for 16 h and diluted with ethanol to achieve absorbance value of 0.7 ± 0.1 at 734 nm. On the other hand, 25 mg of the film sample was dissolved in 5 ml ethanol for extraction. The extracted dilution and ABTS solution (0.1:3, v/v) were mixed and incubated in dark for 10 min at room temperature. The absorbance was read at 734 nm by using spectrophotometer (JASCO, V550, Tokyo, Japan). A Trolox calibration curve (0.2–1.2 mM) was used as a reference to present the ABTS inhibition activity as Trolox equivalent antioxidant capacity (TEAC).

2.7. Structural analysis

2.7.1. Fourier transform infrared spectroscopy (FT-IR)

To elucidate the chemical finger printing, and to identify functional groups of interest in the caseinate films before and after release kinetics, FTIR analysis was conducted by using an infrared spectrometer (Model 100, PerkinElmer, USA) coupled with attenuated total reflectance (ATR). The FT-IR spectra were recorded in the 4000-650 cm^{-1} range using absorbance mode with a resolution of 4 cm^{-1}, and for each spectrum 16 scans were co-added.

2.7.2. Microstructure

The microstructure of the neat caseinate and caseinate films with gallic acid was studied by using scanning electron microscopy (SEM) (ZEISS, EVO, NY, USA). Briefly, film samples (2 × 2 cm^2) were coated with gold by using a vacuum sputter coater before analysis. Then samples were placed on the specimen stage and an accelerating voltage of 20 kV was used during analysis.

2.8. Molecular docking studies

Molecular docking method was used to study interactions between gallic acid and PPO/AO (Zhou et al., 2016). Briefly, the three-dimensional (3D) structure of PPO (PDB ID: 2P3X) was obtained from the RCSB protein data bank (https://www.rcsb.org/), on the other hand, 3D structure of AO was generated by submitting amino acid sequence (FASTA sequence) obtained from NCBI database (https://www.ncbi.nlm.nih.gov/) to the I-TASSER protein server. The 3D conformer of gallic acid was also acquired from Pubchem. For the preparation of proteins, polar hydrogens were added, water molecules were deleted, and they were assumed to be rigid, while for gallic acid all rotatable torsions were activated. Blind dockings were performed by using Autodock Tools (version 1.5.6, The Scripps Research Institute) with spacing of 1 Å, grid box diensions (x-size = 40 Å, y-size = 40 Å, and z-size = 40 Å) and results were analyzed by using Discovery Studio 2021 (BIOVIA, Dassault Systems).

2.9. Statistical analysis

The analysis of variance (ANOVA) was performed to estimate the significant difference ($p < 0.05$) among mean observations (SPSS version 23.0, IL, USA). A total of three replicates were tested during each experiment except for tensile properties, color parameters and thickness of the films (for which seven, five and six replicates were tested respectively).

3. Results and discussion

3.1. Physical properties

3.1.1. Thickness

The thickness of the film samples varied between 0.053 and 0.069 mm and increased significantly ($p < 0.05$) after the addition of guar gum into neat caseinate FFS (Table 1). However, a significant decrease ($p < 0.05$) in film thickness was observed after the incorporation of gallic acid, followed by an increase in thickness values (still lower than control) with increasing concentration of gallic acid. These results can be justified by the small dimension of gallic acid molecule that easily fits in the empty spaces present in the protein network (Parveen et al., 2019). Contrarily, large polyphenolic compounds i.e., tannic acid increase film thickness by entrapping significant amount of air bubbles in protein matrix (Hager et al., 2012).

3.1.2. Water vapor permeability (WVP)

One of the major functions of active antioxidant films is to impede the moisture transfer between the product and its surrounding environment, thus the WVP should be as low as possible to avoid spoilage (Hager et al., 2012). The control caseinate film was highly water permeable and addition of guar gum into caseinate FFS further increased the WVP of the film samples due to its hydrophilic nature. However, upon incorporation of gallic acid the WVP decreased significantly ($p < 0.05$) (a 21% decrease was observed for films with 250 μg/ml gallic acid) from 9.92 to 7.86 × 10^{-11} g $m^{-1}s^{-1}$ Pa^{-1} (Table 1), because gallic acid induced interactions with polymeric network of caseinate/gum resulting into more compact film impeding water transfer across film. Another reason is the possible hydrophobic (Pi-alkyl) interactions of gallic acid with casein fractions. Gallic acid might also cover the hydrophilic domains present on the protein surface, as a result trapping small water molecules resulting in a decrease in WVP. Furthermore, as reported by Irissin-Mangata et al. (2000), interactions between gallic acid and polymer can also reduce the availability of hydrophilic groups (hydroxyl and amine) for interaction with water molecules. However, an increase in WVP was observed upon increasing the concentration of gallic acid beyond 250 μg ml^{-1}, due to disruption of intermolecular interactions among polypeptide chains caused by increased gallic acid concentration.

3.1.3. Water solubility and surface hydrophobicity

The water solubility of a packaging film is an important indicator of its resistance to water (Yadav et al., 2021). The control films were highly water soluble because of their hydrophilic nature. Similarly, upon incorporation of gallic acid the water solubility significantly increased ($p < 0.05$) from 58% to 63% (Table 1) due to the hydrophilic nature of the phenolic compound. Our results are in accordance with Rui et al. (2017), who observed an increase in water solubility of chitosan films with increase in grafting of films with gallic acid due to presence of hydrophilic moieties. However, this drawback of hydrophilicity can be resolved by sandwiching the caseinate films between two hydrophobic polycaprolactone films by hot pressing to protect them from direct contact with water and moisture transfer as described by Bayer et al. (2022) for poly lactic acid (PLA) films enriched with carminic acid.

The WCA increases with increasing surface hydrophobicity. The neat caseinate film had a WCA of ~61.5°, a significant decrease ($p < 0.05$) in surface hydrophobicity was observed after the incorporation of both guar gum and gallic acid into the FFS due to binding of more hydrophilic groups (amino and carboxyl) on the surface of polymeric matrix with water. Generally, materials with WCA <90° are considered hydrophilic while materials having WCA >90° are considered hydrophobic. These results are in agreement with some recent literature, in which authors reported a decrease in surface hydrophobicity upon incorporation of gallic acid into FFS due to increase in polar groups (Yadav et al., 2021).

Table 1
Thickness, water vapor permeability, water solubility, surface hydrophobicity and mechanical properties of the films.

Sample	Thickness (mm)	WVP ($\times 10^{-11}$ g m^{-1}·s^{-1} Pa^{-1})	WS (%)	WCA (°)	TS (MPa)	EAB (%)	EM (MPa)
C	0.066 ± 0.007^{ab}	9.304 ± 0.21^{b}	54.08 ± 2.10^{b}	61.5 ± 3.04^{a}	n.a	n.a	n.a
C + G	0.069 ± 0.006^{a}	9.92 ± 0.05^{a}	58.29 ± 0.28^{ab}	54 ± 3.60^{abc}	0.31 ± 0.05^{a}	6.34 ± 1.99^{a}	15.61 ± 1.65^{a}
C + G + GA I	0.053 ± 0.009^{c}	7.94 ± 0.05^{d}	60.95 ± 1.63^{ab}	58.16 ± 2.25^{ab}	0.31 ± 0.07^{a}	9.36 ± 3.06^{a}	15.18 ± 4.75^{a}
C + G + GA II	0.057 ± 0.010^{bc}	7.86 ± 0.18^{d}	61.69 ± 3.58^{b}	51.83 ± 3.61^{bc}	0.33 ± 0.10^{a}	6.90 ± 2.90^{a}	12.72 ± 3.21^{a}
C + G + GA III	0.063 ± 0.007^{abc}	8.88 ± 0.20^{c}	63.20 ± 3.74^{a}	48.10 ± 2.25^{c}	0.33 ± 0.08^{a}	7.14 ± 1.77^{a}	13.18 ± 2.58^{a}

Different superscript letters (a-d) within a column show significant differences ($p < 0.05$) among mean observations. Whereas C = sodium caseinate, C+G = sodium caseinate + guar gum, C + G + GAI = sodium caseinate + guar gum + gallic acid 60 μg ml^{-1} of the FFS, C + G + GAII = sodium caseinate + guar gum + gallic acid 250 μg ml^{-1} of the FFS, and C + G + GAIII = sodium caseinate + guar gum + gallic acid 650 μg ml^{-1} of the FFS.

3.1.4. Mechanical properties

The results of mechanical properties are presented in Table 1. The TS of the films improved slightly but non-significantly ($p > 0.05$) after the addition of gallic acid into the FFS. This could be due to interaction of polymeric molecules with gallic acid by a protein-phenol interaction, which led to the formation of larger molecules and improved the TS. Limpisophon and Schleining (2017) similarly suggested that gelatin prevented the self-association of gallic acid in the FFS and after the drying process gallic acid was closely located to a peptide side-chain suggesting interaction between protein and polyphenol. This is also an indication of intermolecular hydrogen bonding between NH_3^+ backbone of the polypeptide and OH^- group of the polyphenol, which leads to decrease in free volume of the matrix and chain mobility (Sun et al., 2014). These results can also be correlated with the non-significant ($p > 0.05$) increase and decrease in EAB and EM values respectively of films with increasing concentration of gallic acid (from 60 μg/ml to 650 μg/ml). These results suggest that gallic acid might be located more on the surface of the film rather than inserted in the film matrix. However, this polyphenol effect on the mechanical properties of the film is not always similar and it depends upon polyphenol type and size, the nature of the polymer and processing conditions (Rani et al., 2021).

3.1.5. Optical properties

Optical properties are an essential characteristic of a packaging film related to its functionality which has great impact on the appearance of the films; ultimately depending upon consumer preferences and product applicability. Table 2. shows color parameters and opacity values for bioactive films based on sodium caseinate. Generally, caseinate and caseinate/gum films are relatively whitish (with ΔE values 1.6–2) as expected and reported in literature (Alizadeh-Sani et al., 2020). In our study, we observed a significant decrease in lightness (L) and WI index values of the films with increasing concentration of gallic acid from 60 to 650 μg ml^{-1}. It has been reported in literature that gallic acid films are relatively white and with high WI (Zhao and Saldaña, 2019), but we observed a significant increase in ΔE values (from 1.96 to 5) with increasing gallic acid concentration. This can be justified by the use of alkaline conditions (i.e., Tris buffer in this case), which allows gallic acid to absorb oxygen in large amount and forming larger molecules, causing a change in color of FFS from white to dark brown, green or grey (Fig. S1) and ultimately producing films with slight yellowish appearance (Pant et al., 2017) which also affected b* (yellowness) parameter of the films. Generally, the oxygen scavenging ability of gallic acid is dependent on the autoxidation of gallic acid at alkaline pH. The type and quantity of oxidation products change with pH and a pH above 8 is necessary to produce dark-colored reaction products (affecting both L* and b* values of the film). Thus, pH-dependent deprotonation of gallic acid can play a vital role in the possibility of using the gallic acid films as indicators of basic-pH (Pant et al., 2019).

Table 2
Optical properties of the film samples.

Sample	L*	a*	b*	ΔE	WI (%)	Opacity
C	95.58 ± 0.34^{a}	0.038 ± 0.16^{a}	1.89 ± 0.89^{a}	1.6 ± 0.24^{c}	95.14 ± 0.48^{a}	1.65 ± 0.04^{b}
C + G	95.41 ± 0.48^{a}	0.046 ± 0.08^{a}	2.73 ± 1.02^{a}	1.96 ± 0.60^{bc}	94.6 ± 0.58^{ab}	1.71 ± 0.07^{b}
C + G + GA I	93.71 ± 0.94^{b}	0.082 ± 0.06^{a}	3.95 ± 0.81^{a}	3.88 ± 1.15^{ab}	92.55 ± 1.03^{bc}	1.94 ± 0.05^{a}
C + G + GA II	94.21 ± 0.89^{ab}	0.044 ± 0.25^{a}	4.09 ± 2.25^{a}	3.91 ± 1.54^{ab}	92.7 ± 1.33^{bc}	1.92 ± 0.01^{a}
C + G + GA III	93.13 ± 1.14^{b}	−0.008 ± 0.44^{a}	4.66 ± 2.17^{a}	5.0 ± 1.70^{a}	91.54 ± 1.52^{c}	1.94 ± 0.01^{a}

Different superscript letters (a-c) within a column show significant differences ($p < 0.05$) among mean observations. Whereas C = sodium caseinate, C+G = sodium caseinate + guar gum, C + G + GAI = sodium caseinate + guar gum + gallic acid μg.ml^{-1} of the FFS, C + G + GAII = sodium caseinate + guar gum + gallic acid 250 μg ml^{-1} of the FFS, and C + G + GAIII = sodium caseinate + guar gum + gallic acid 650 μg ml^{-1} of the FFS.

On the other hand, control films were less opaque than films loaded with gallic acid. The opacity of the packaging films increased significantly ($p < 0.05$) after the incorporation of gallic acid into the mix, however, no significant influence of gallic acid concentration was observed on the opacity values (which ranged between 1.92 and 1.94). Similarly, percentage transmittance of the film samples was determined by scanning the film samples at 300–700 nm using UV-VIS spectroscopy (Fig. S2). The control film (sodium caseinate + guar gum) samples were very transparent with percentage transmittance of 20% and 85% in both UV and visible regions respectively due to presence of aromatic amino acids in the polypeptide chain of casein (Bonilla and Sobral, 2017). However, after incorporation of gallic acid the transmittance of light (both in UV and visible regions) decreased significantly ($p < 0.05$) as compared to control. In fact, gallic acid has an aromatic ring, which displays anti-UV properties in the UV-region (280–320 nm) by absorption (Luo et al., 2021). A substantial blocking of light both in UV and visible region can reduce to risk of activation of oxidative enzymes, which could lead to oxidation of the produce, loss of nutritional quality, and reduction in shelf life.

3.2. Release kinetics of gallic acid

The migration test was performed according to European Standard EN 13130–200522 to elucidate the release of gallic acid from the packaging materials into the simulant. Fig. 1 shows the release of gallic acid at various concentrations from the packaging film into the food simulant (95% ethanol). As excepted, there was a significant difference in the amount of gallic acid release with increasing concentration in the film ($p < 0.05$). During the first 3 h, the concentration of gallic acid released into the simulant varied between 9.6 and 10.7 μg ml^{-1} (for all the samples) followed by a two-fold increase in concentration in the next 2 h. The highest concentration of gallic released into the food simulant was observed at 192 h of incubation (40.1 μg ml^{-1} for GAI, 79.8 μg ml^{-1} for GAII, and 182 μg ml^{-1} for GAIII), followed by a slight decrease in the concentration, and it is safe to assume that equilibrium has reached at this point. This trend was similar for all concentrations of gallic acid. The enhanced porosity of the film might be the reason for the concentration

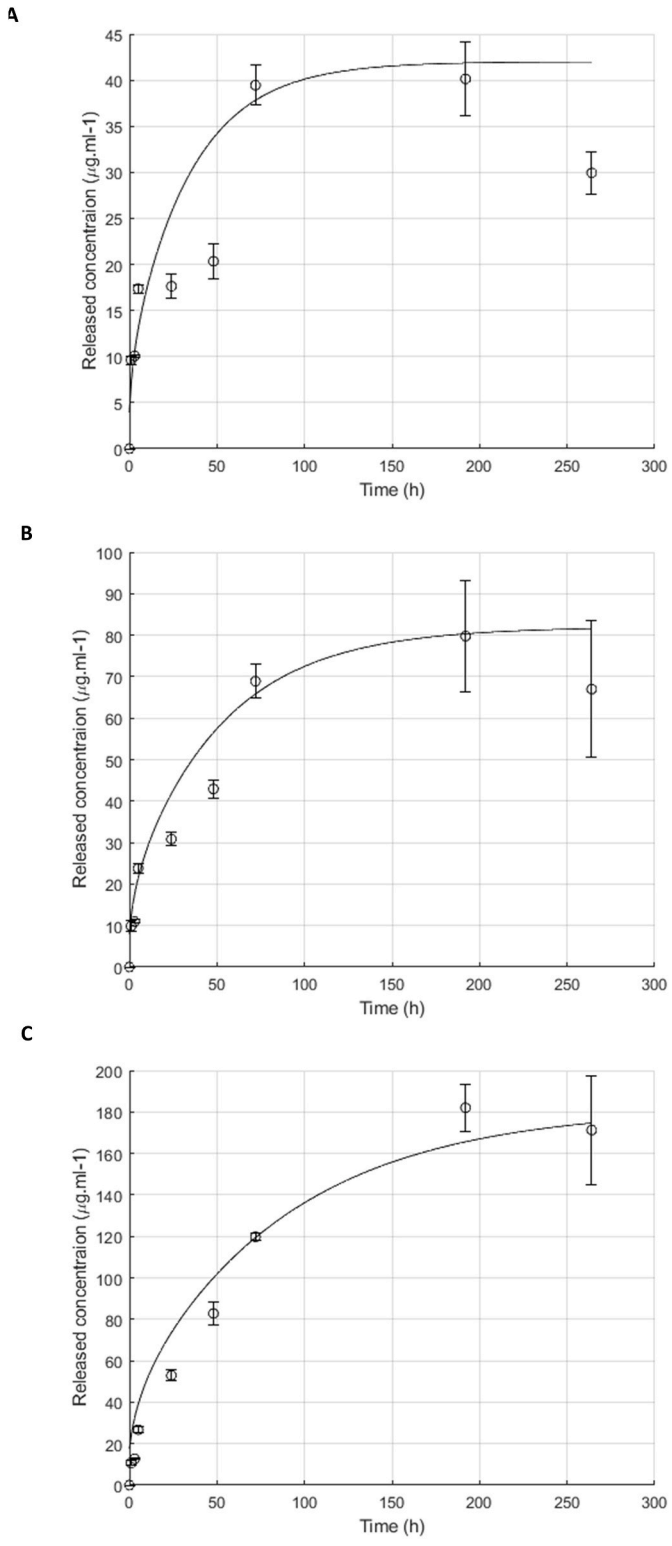

Fig. 1. Release kinetics and mathematical modelling of release behavior of gallic acid (Where **A** = sodium caseinate + guar gum + gallic acid 60 μg ml^{-1} of the FFS, **B** = sodium caseinate + guar gum + gallic acid 250 μg ml^{-1} of the FFS, and **C** = sodium caseinate + guar gum + gallic acid 650 μg ml^{-1} of the FFS; also "o" represents experimental while solid line "-" represents predicted values).

dependency of gallic acid release from the film matrix, as similarly reported by (Marvdashti et al., 2019). In our study, ~67% (GAI), 32% (GAII), and 30% (GAIII) gallic acid leeched out into the food simulant. Perhaps, the influence of film thickness is more evident on the release kinetics of the bioactive compounds at lower concentrations (since in this case we had two times more release from the film with lowest gallic acid concentration). Swelling controlled model can be used to describe this release behavior: when the food simulant enters the film matrix it dissolves the bioactive compound, causing its release from matrix, which causes the polymer to swell, until equilibrium is reached followed by relaxation of the polymer matrix which is time dependent (Paarakh et al., 2018). Another reason for the increased release of gallic acid from the films might be due to its affinity towards ethanol, in fact gallic acid is less soluble in water than ethanol (Noubigh et al., 2012). Similar results were observed by Rubilar et al. (2017), authors reported higher release of gallic acid (>75%) from the chitosan films due to higher temperatures and lower gallic acid concentration (3.8 μg ml^{-1}) used, while the higher gallic acid concentration (6.5 μg ml^{-1}) had lower release values (<55%) even when incubating at 45 °C. Furthermore, admissible daily intake (ADI) has not been established yet for gallic acid, however, for propyl gallate (an ester of gallic acid) it is 0.2 mg kg^{-1} (EFSA, 2014). If we assume that gallic acid has the same ADI, thus for an adult of 65 kg the limit is 13 mg. Considering that same adult eats 1 kg of food covered with conventional film as lid (1 g weight) with different gallic acid concentrations (GAI, II and III) the released amount would be lower than ADI (~1, 2 and 4.5 mg respectively).

3.3. Mathematical modelling

A mathematical model is useful in designing an active package by elucidating the release behavior of a bioactive especially during shelf-life. In this study, Fick's model was used for the fitting of experimental data to describe the release of different concentrations of gallic acid from the film, and to estimate the capacity of Fick's Law to describe the release behavior. The mathematical models used to fit the experimental data are shown in Fig. 1. For film sample GAI, the diffusivity was observed to be 8.10×10^{-12} m^2 s^{-1} with RMSE and coefficient of correlation (R^2) values of 0.10 and 0.83 respectively and a released amount of ~66.7% compared to 66.8% of the experimental one. Slower diffusion coefficients (6.23 and 4.5×10^{-12} m^2 s^{-1}) were observed for GAII and GAIII films respectively with RMSE and R^2 ranging between 0.03–0.02 and 0.95–0.99 respectively with reduced released values (<35%). This could be because with increasing gallic acid concentration in the film, the hydrophilicity of the film samples increased, which led to slower diffusion coefficients and released amount at higher gallic acid concentration in a hydrophobic medium. Similarly, Dede and Lokumcu Altay (2019) demonstrated higher diffusion coefficient values for limonene encapsulated by polyvinyl alcohol and gelatin in water as compared to ethanol due to hydrophilic behavior of the polymers which led to easy diffusion and bulk release into aquatic medium. Additionally, differences in diffusivity values can also be explained in terms of interaction of bioactive with polymeric chains and its solubility in food simulant, mainly depending on its polarity (Requena et al., 2017). Our results were in accordance with those found in literature (Marvdashti et al., 2019). Furthermore, the experimental data was sufficiently described by Fick's model, suggesting good linearity and excellent fitting of the experimental data with the predicted one (Rubilar et al., 2017). Rubilar et al. (2017) similarly reported slower D values for gallic acid release into bi-distilled water from chitosan films ranging between $1.8–6.1 \times 10^{-14}$ m^2 s^{-1} at low temperatures, while a faster diffusivity ($1.9–5.4 \times 10^{-13}$ m^2 s^{-1}) for films incubated at highest temperature. The highest K value (>2) was observed for GAI film samples which was significantly different than other two samples (<0.5) (Table S2) indicating that at lower concentration (<650 μg ml^{-1}) gallic acid has better affinity for simulant than the film, however, several factors i.e., chemical nature, solubility, polarity and affinity of the migrant towards polymer affects the value of K (Suppakul et al., 2003).

3.4. Antioxidant activity

The DPPH radical scavenging activity is based on the reduction of DPPH radical (purple color) in the presence of a hydrogen donating antioxidant into yellow colored compound. The DPPH radical scavenging activity of food simulant solutions containing gallic acid is presented in Fig. 2A. The antioxidant activity increased significantly for all the samples followed by a decrease (after 72 h). The DPPH radical scavenging activity of GAI ranged from 37 to 53%, for GAII from 38 to 77% and for GAIII from 40 to 80%. The highest DPPH radical scavenging activity was observed for food simulant containing films samples GAIII (~80%), which makes the gallic acid films useful as an effective antioxidant package despite its hydrophilic nature. These values were similar to those found in recent literature, because low degree of cross-linking due to the absence of coupling agents made the films leach more gallic acid into the simulant. Gallic acid neutralizes the DPPH radical by HAT mechanism owing to the loss of proton and stabilization of the charge by the surrounding groups (the lower bond dissociation energy of O–H in –COOH group of gallic acid favors H-atom-transfer). Upon reaction, loss of one the aromatic hydroxyl groups occurred, and the remaining protons were delocalized probably because they were in ortho configuration, however, no quinone were formed during the interaction (López-Martínez et al., 2015). Furthermore, a decrease in antioxidant activity at the end is an indication that few DPPH radicals were available to interact with hydroxyl groups of gallic acid (Zarandona et al., 2020) or maybe gallic acid was not able to act as scavenger because it was oxidized.

The antioxidant activity of control film samples was extremely low and ranged between 0.05 and 0.06 TEAC (mM). On the other hand, a significant ($p < 0.05$) increase in antioxidant activity was observed after incorporation of gallic acid into the FFS and with increasing concentration of gallic acid in the film matrix (from 60 μg/ml to 650 μg/ml) (Fig. 2B). The highest antioxidant activity was observed for GAIII film samples at ~1.27 TEAC (mM). Gallic acid can scavenge free radicals by causing the reduction of the $ABTS^{+}$ radicals by one or more mechanisms, thus exhibiting high antioxidant capacity (Xie et al., 2014). The differences in antioxidant activity of all film samples can also be attributed to the differences in the structure and water solubility (Rui et al., 2017).

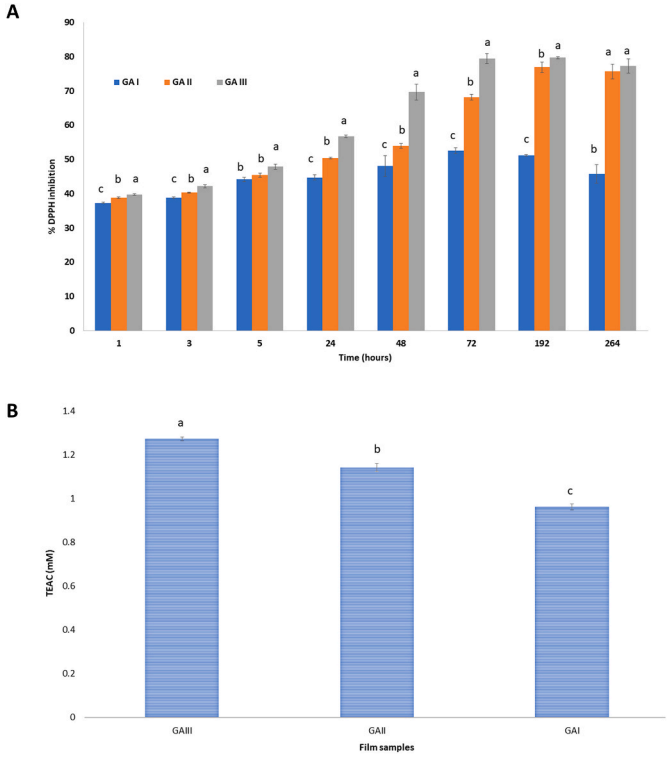

Fig. 2. Antioxidant activity of the A = food simulant solutions and B = films (Different superscript letters (a–c) above bars show significant differences ($p < 0.05$) among mean observations. Whereas C + G + GAI = sodium caseinate + guar gum + gallic acid 60 μg ml^{-1} of the FFS, C + G + GAII = sodium caseinate + guar gum + gallic acid 250 μg ml^{-1} of the FFS, and C + G + GAIII = sodium caseinate + guar gum + gallic acid 650 μg ml^{-1} of the FFS).

3.5. Structural characteristics

3.5.1. FT-IR

The chemical finger printing of all the film samples is shown in Fig. 3. Peaks of ~1050, 1540, 1630, 2960, and 3270 cm^{-1} were found in all film samples. The broad peaks around 1630 (amide-I and 3270 cm^{-1} (amide-A) were due to stretching and bending vibrations of the –OH functional groups. The peak at 2960 cm^{-1} was due to stretching vibration of the C–H group associated with the ring of methane hydrogen atoms (Picchio et al., 2018). The peaks between ~1630 and 1700 cm^{-1} can be associated with stretching vibration of C═O in aldehyde and amide functional groups, it can also indicate the absorption of water by guar gum (Alizadeh-Sani et al., 2020). The hydrogen bonding between casein and guar gum was confirmed by the broadband between 3000 and 3500 cm^{-1}. Peaks between ~1040 and 1100 cm^{-1} were an indication of C–O pyranose stretching vibration in guar gum, structural vibrations in glycoside bond, amino group stretching (C–N), formation of ether bonds (C–*O*–C), and presence of glycerol in the film matrix. The peaks at ~1530 (amide-II) and 1240 cm^{-1} (amide-III) can be attributed to N–H bending and N–H and C–N stretching vibrations respectively (Picchio et al., 2018). After the incorporation of gallic acid into the films the peak positions shifted to a higher wavenumber in amide-A (from 3274 to 3277 cm^{-1}), furthermore, the absorption band at 1633 cm^{-1} corresponding to amide-I is also indicating overlapping carboxylic acid group of gallic acid, confirming the formation of hydrogen bond between casein and gallic acid at basic pH (Leceta et al., 2018). Furthermore, the C–C stretching mode of aromatics at 1615 cm^{-1} and C–O stretching at 1015 cm^{-1} have also been reported to be linked with the presence of gallates in the films (Quilez-Molina et al., 2020). On the other hand, additional peaks at 3074-3075 cm^{-1} were observed in the samples after release (Table S1), indicating stretching of aromatic C–H group confirming the release of gallic acid from the films. This phenomenon was also confirmed by the shifting of wavenumber in amide-I region to a lower number from 1633 to 1629 cm^{-1} and stretching of C–O, C–*O*–C and C–N group (shifting of wavenumber to a higher wavelength from 1047 to 1074 cm^{-1}) for all the film samples after release. The stretching of C–N group could be an indication of two things, a) detachment of gallic acid from polymeric chains due to cleavage of linkages, or b) formation of hydrogen bonding between polymer and solvent molecules which shifted the frequency to higher wavenumbers (Huang et al., 2003).

3.5.2. SEM

The SEM micrographs displaying the surface microstructure of the control and composite films containing gallic acid are shown in Fig. 5. The neat caseinate films were smooth surfaced, without any cracks and homogenous. After the addition of guar gum and gallic acid into caseinate FFS, the roughness of the film samples increased with slight protuberance, indicating formation of hydrogen bonds between hydrophilic compounds (Fig. 4A and B). Moreover, as reported by Parveen et al. (2019) an increment of roughness can be also due to agglomeration on the surface due to covalent and non-covalent interactions between gallic acid and polypeptide chains. A low degree of heterogeneity was observed in film sample with highest level of GA (GAIII) as compared to the films with lower levels of gallic acid (Fig. 4E) (Limpisophon and Schleining, 2017). Presence of cracks and pores in the gallic acid film sample (GAIII) were also observed. The higher content of gallic acid

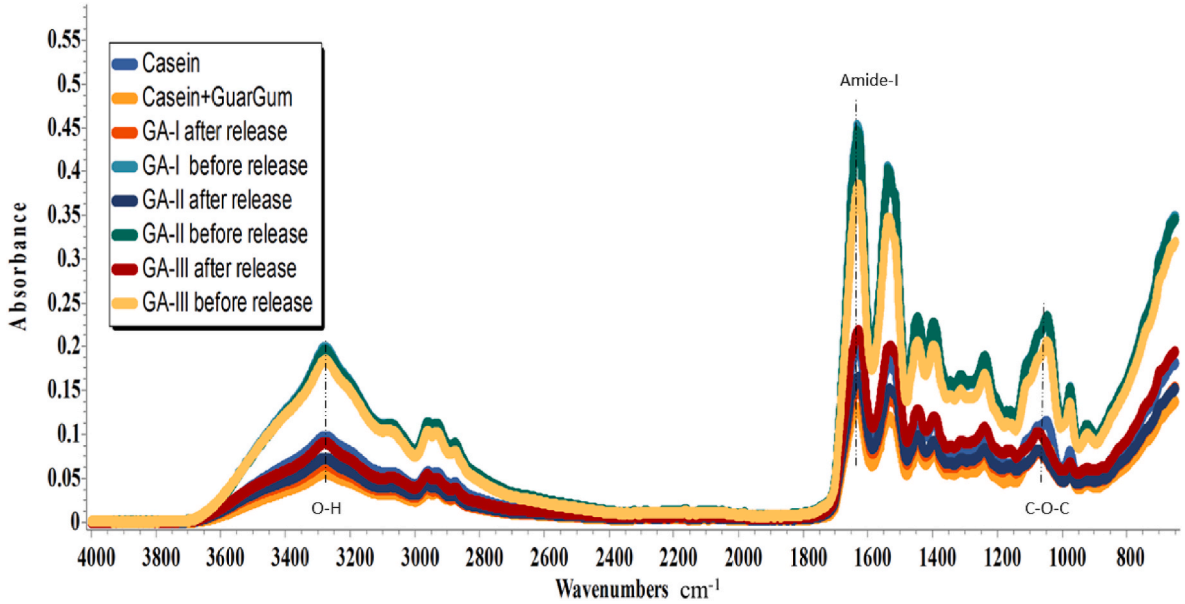

Fig. 3. Chemical fingerprinting of neat and composite films (Where C = sodium caseinate, C+G = sodium caseinate + guar gum, C + G + GAI = sodium caseinate + guar gum + gallic acid 60 μg ml^{-1} of the FFS, C + G + GAII = sodium caseinate + guar gum + gallic acid 250 μg ml^{-1} of the FFS, and C + G + GAIII = sodium caseinate + guar gum + gallic acid 650 μg ml^{-1} of the FFS.

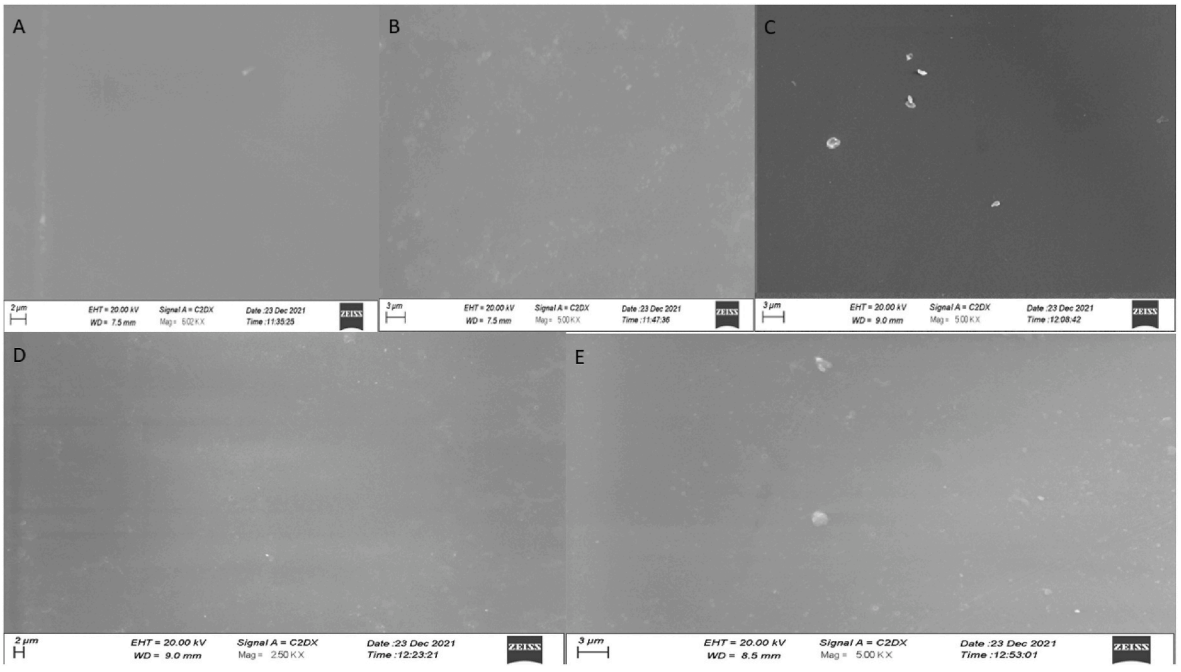

Fig. 4. Microstructure of neat and composite films with gallic acid (Where A = sodium caseinate, B = sodium caseinate + guar gum, C = sodium caseinate + guar gum + gallic acid 60 μg ml^{-1} of the FFS, D = sodium caseinate + guar gum + gallic acid 250 μg ml^{-1} of the FFS, and E = sodium caseinate + guar gum + gallic acid 650 μg ml^{-1} of the FFS).

restricted polymeric chain movement in polymeric matrix due to the entanglements. Our results are in agreement with the concept that surface properties directly influence the barrier properties of the film (Sun et al., 2014). Furthermore, the surface roughness and surface energy influence the surface hydrophobicity. The surface hydrophobicity is a factor which may influence the molecular transport through membrane and thin polymeric structures including films (Jamshidian et al., 2012).

3.6. Molecular modelling

The molecular modelling is an innovative approach to study the interactions between a protein and a ligand. The inactivation of oxidizing enzymes (i.e., PPO and AO) is of high importance to preserve the quality of minimally processed foods. Since polyphenols have been reported to inactivate the oxidizing enzymes (Khan et al., 2021a,b), in this study, we used molecular docking to study the interactions between polyphenol and oxidizing enzymes to design an effective active releasing system. Fig. 5 shows the binding affinity of gallic acid with both PPO and AO. We

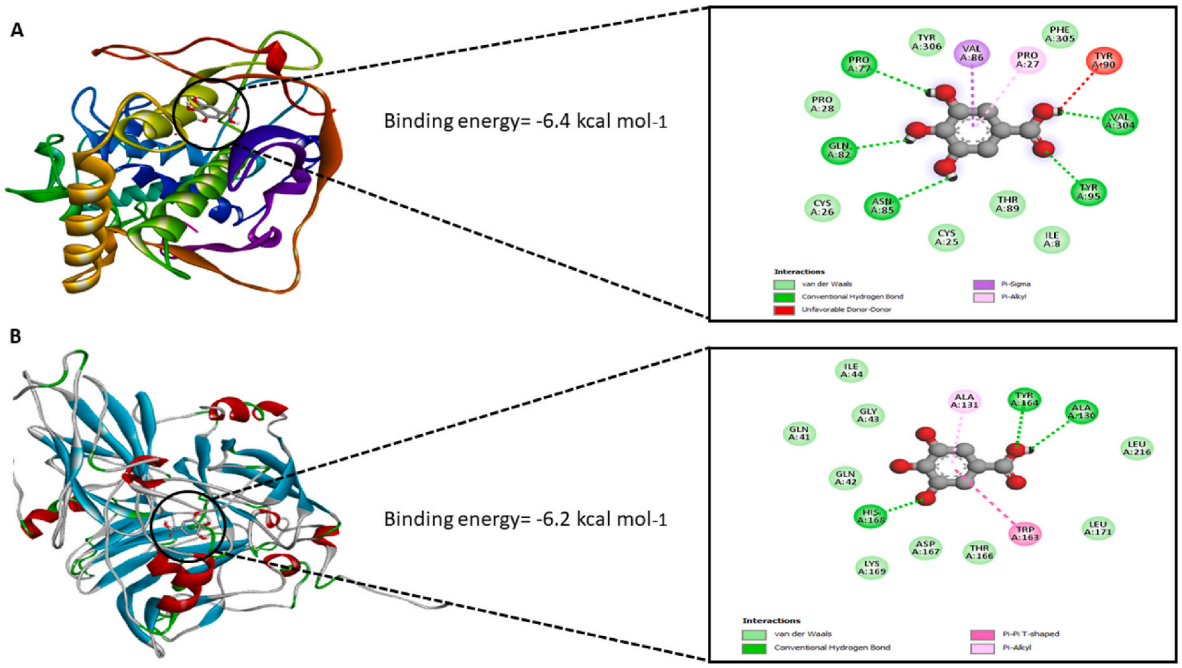

Fig. 5. Molecular docking of gallic acid with A) Polyphenol oxidase, and B) Ascorbate oxidase.

observed excellent binding affinity of gallic acid at −6.4 and −6.2 kcal mol^{-1} for PPO and AO respectively due the hydrophilic nature of the ligand and which were comparable to the binding energies reported in literature for PPO of benzoic and cinnamic acids (−6.1 and −6.4 kcal mol^{-1}, respectively) (Sun et al., 2021). Similarly, top molecular docking suggested formation of five hydrogen bonds at the hydrogen of hydroxyl group of gallic acid with respective amino acids of PPO: PRO 77, GLN 82, ASN 85, TYR 95 and VAL 304 in the hydrophobic pocket. Furthermore, one Pi-Sigma and one hydrophobic Pi-alkyl interaction was found between benzene ring of gallic acid and VAL 86 and PRO 27 respectively, other notable interactions involved van der Waals (Fig. 5A). Molecular docking of gallic acid with AO suggested lesser hydrogen bonding as compared to PPO, thus less binding affinity. Hydrogen interactions were observed at ALA 130, TYR 164, and HIS 168. Benzene ring of gallic acid displayed hydrophobic Pi-alkyl and Pi-Pi-T shaped interactions with following amino acids of AO respectively: ALA 131 and TRP 163. Gallic acid have the potential to inhibit the activity of both PPO and AO by binding near the active site (especially formation of hydrogen bonds could reduce the overall polarity of the enzyme), causing the rearrangement of the secondary structure of PPO/AO, ultimately avoiding the formation of oxidation product as suggested by (Sun et al., 2021; Zhou et al., 2016). In addition, chelating reaction between polyphenols and Cu atom of oxidative enzymes can also induce inhibition of oxidative enzymes by affecting the properties of trinuclear cluster (Gaspard et al., 1997). Thus, addition of gallic acid in releasing packaging systems can lead to inactivation of these enzymes causing the preservation of the nutritional quality of minimally processed produce.

4. Conclusion

The barrier properties of sodium caseinate based films (both against light and water permeability) were improved after the incorporation of gallic acid in film matrix. However, hydrophobicity of the films decreased. Sodium caseinate based films controlled the release of gallic acid into the food simulant. The film samples with lowest gallic acid concentration displayed highest release values due to their less hydrophilic nature. The release of gallic acid from sodium caseinate films was studied by using mathematical models. The films with lowest gallic acid concentration displayed fastest diffusion coefficient value (8.1×10^{-12} m^2 s^{-1}). Despite the hydrophilic nature of the packaging material, the high antioxidant potential (~80% DPPH inhibition) of the films (with higher gallic acid content) can make them useful for the packaging purposes. The molecular docking of gallic acid against PPO and AO suggested possible inhibition of both the enzymes by binding near the active site in the hydrophobic pocket, causing the rearrangement of the secondary structure of PPO and AO. However, this is an initial computational trial as far as enzyme inactivation is concerned. The detailed enzyme inhibition mechanism should be studied both *in-vitro* and real time products to better understand the dynamics of inactivation. The mathematical and molecular modelling studies can serve as an effective tool for designing efficient biodegradable active releasing packaging forms.

Authorship statement

M. R. Khan; Acquisition of data; Data analysis and/or interpretation; Drafting of manuscript and/or critical revision S. Volpe; Acquisition of data; Data analysis and/or interpretation; Drafting of manuscript and/or critical revision Acquisition of data; Data analysis and/or interpretation; Drafting of manuscript and/or critical revision E. Salucci: Data analysis and/or interpretation; B. S., Muhammad Data analysis and/or interpretation; Drafting of manuscript and/or critical revision E. Torrieri Conception and design of study; Data analysis and/or interpretation; Drafting of manuscript and/or critical revision; Approval of final version of manuscript.

Declaration of competing interest

The authors declare no conflict of interest.

Acknowledgements

The PhD fellowship of the first author is supported by MIUR. The research activity is also supported by the European Union's Horizon 2020 Project No. 817936. IPCB-CNR is kindly acknowledged for their support in FT-IR analysis.

Appendix A. Supplementary data

Supplementary data to this article can be found online at https://doi.org/10.1016/j.jfoodeng.2022.111190.

References

Alizadeh-Sani, M., Rhim, J.W., Azizi-Lalabadi, M., Hemmati-Dinarvand, M., Ehsani, A., 2020. Preparation and characterization of functional sodium caseinate/guar gum/TiO2/cumin essential oil composite film. Int. J. Biol. Macromol. 145, 835–844.

Asgher, M., Qamar, S.A., Bilal, M., Iqbal, H.M., 2020. Bio-based active food packaging materials: sustainable alternative to conventional petrochemical-based packaging materials. Food Res. Int. 137, 109625.

Bayer, G., Shayganpour, A., Zia, J., Bayer, I.S., 2022. Polyvinyl alcohol-based films plasticized with an edible sweetened gel enriched with antioxidant carminic acid. J. Food Eng. 323, 111000.

Benbettaieb, N., Cox, R., Gilbert, M., Debeaufort, F., 2021. How the temperature and salt content of food simulant affect the release of tyrosol or phenolic acids from bioactive films? Future Foods, 100040.

Benbettaïeb, N., Mahfoudh, R., Moundanga, S., Brachais, C.H., Chambin, O., Debeaufort, F., 2020. Modeling of the release kinetics of phenolic acids embedded in gelatin/chitosan bioactive-packaging films: influence of both water activity and viscosity of the food simulant on the film structure and antioxidant activity. Int. J. Biol. Macromol. 160, 780–794.

Bonilla, J., Sobral, P.J., 2017. Antioxidant and physicochemical properties of blended films based on gelatin-sodium caseinate activated with natural extracts. J. Appl. Polym. Sci. 134 (7).

Cavalcante, T.A.B.B., dos Santos Funcia, E., Gut, J.A.W., 2021. Inactivation of polyphenol oxidase by microwave and conventional heating: investigation of thermal and non-thermal effects of focused microwaves. Food Chem. 340, 127911.

Crank, J., 1979. The Mathematics of Diffusion. Oxford university press.

Dede, S., Lokumcu Altay, F., 2019. Nanofibre encapsulation of limonene and modelling its release mechanisms. Acta Aliment. 48 (1), 56–64.

Dede, S., Sadak, O., Didin, M., Gunasekaran, S., 2022. Basil oil-loaded electrospun biofibers: edible food packaging material. J. Food Eng. 319, 110914.

Di Giuseppe, F.A., Volpe, S., Cavella, S., Masi, P., Torrieri, E., 2022. Physical properties of active biopolymer films based on chitosan, sodium caseinate, and rosemary essential oil. Food Packag. Shelf Life 32, 100817.

Domínguez, R., Barba, F.J., Gómez, B., Putnik, P., Kovačević, D.B., Pateiro, M., et al., 2018. Active packaging films with natural antioxidants to be used in meat industry: a review. Food Res. Int. 113, 93–101.

EFSA Panel on Food, 2014. Scientific Opinion on the re-evaluation of propyl gallate (E 310) as a food additive. EFSA J. 12 (4), 3642.

Gaspard, S., Monzani, E., Casella, L., Gullotti, M., Maritano, S., Marchesini, A., 1997. Inhibition of ascorbate oxidase by phenolic compounds. Enzymatic and spectroscopic studies. Biochemistry 36 (16), 4852–4859.

Hager, A.S., Vallons, K.J., Arendt, E.K., 2012. Influence of gallic acid and tannic acid on the mechanical and barrier properties of wheat gluten films. J. Agric. Food Chem. 60 (24), 6157–6163.

Hanani, Z.N., Yee, F.C., Nor-Khaizura, M.A.R., 2019. Effect of pomegranate (Punica granatum L.) peel powder on the antioxidant and antimicrobial properties of fish gelatin films as active packaging. Food Hydrocolloids 89, 253–259.

Huang, C.Y., Wang, T., Gai, F., 2003. Temperature dependence of the CN stretching vibration of a nitrile-derivatized phenylalanine in water. Chem. Phys. Lett. 371 (5–6), 731–738.

Irissin-Mangata, J., Bauduin, G., Boutevi, B., 2000. Bilayer films composed of wheat gluten film and UV-cured coating: water vapor permeability and other functional properties. Polym. Bull. 44 (4), 409–416.

Jamshidian, M., Tehrany, E.A., Cleymand, F., Leconte, S., Falher, T., Desobry, S., 2012. Effects of synthetic phenolic antioxidants on physical, structural, mechanical and barrier properties of poly lactic acid film. Carbohydr. Polym. 87 (2), 1763–1773.

Khan, M.R., Di Giuseppe, F.A., Torrieri, E., Sadiq, M.B., 2021a. Recent advances in biopolymeric antioxidant films and coatings for preservation of nutritional quality of minimally processed fruits and vegetables. Food Packag. Shelf Life 30, 100752.

Khan, M.R., Volpe, S., Valentino, M., Miele, N.A., Cavella, S., Torrieri, E., 2021b. Active casein coatings and films for perishable foods: structural properties and shelf-life extension. Coatings 11 (8), 899.

Khan, M.R., Volpe, S., Sadiq, M.B., Giannino, F., Torrieri, E., 2022. Correlating in silico elucidation of interactions between hydroxybenzoic acids and casein with in vitro release kinetics for designing food packaging. Food Packag. Shelf Life 32, 100859.

LakshmiBalasubramaniam, S., Howell, C., Tajvidi, M., Skonberg, D., 2022. Characterization of novel cellulose nanofibril and phenolic acid-based active and hydrophobic packaging films. Food Chem. 374, 131773.

Leceta, I., Urdanpilleta, M., Zugasti, I., Guerrero, P., de la Caba, K., BIOMAT Research Group, 2018. Assessment of gallic acid-modified fish gelatin formulations to optimize the mechanical performance of films. Int. J. Biol. Macromol. 120, 2131–2136.

Limpisophon, K., Schleining, G., 2017. Use of gallic acid to enhance the antioxidant and mechanical properties of active fish gelatin film. J. Food Sci. 82 (1), 80–89.

López-Martínez, L.M., Santacruz-Ortega, H., Navarro, R.E., Sotelo-Mundo, R.R., González-Aguilar, G.A., 2015. A 1H NMR investigation of the interaction between phenolic acids found in mango (Manguifera indica cv Ataulfo) and papaya (Carica papaya cv Maradol) and 1, 1-diphenyl-2-picrylhydrazyl (DPPH) free radicals. PloS One 10 (11), e0140242.

Luo, Y., Wu, Y., Wang, Y., Yu, L.L., 2021. Active and robust composite films based on gelatin and gallic acid integrated with microfibrillated cellulose. Foods 10 (11), 2831.

Luzi, F., Pannucci, E., Santi, L., Kenny, J.M., Torre, L., Bernini, R., Puglia, D., 2019. Gallic acid and quercetin as intelligent and active ingredients in poly (vinyl alcohol) films for food packaging. Polymers 11 (12), 1999.

Manzocco, L., Panozzo, A., Nicoli, M.C., 2013. Inactivation of polyphenoloxidase by pulsed light. J. Food Sci. 78 (8), E1183–E1187.

Marvdashti, L.M., Yavarmanesh, M., Koocheki, A., 2019. Controlled release of nisin from polyvinyl alcohol-Alyssum homolocarpum seed gum composite films: Nisin kinetics. Food Biosci. 28, 133–139.

Noubigh, A., Mgaidi, A., Abderrabba, M., 2012. Solubility of gallic acid in liquid mixtures of (ethanol+ water) from (293.15 to 318.15) K. J. Chem. Thermodyn. 55, 75–78.

Núñez-Flores, R., Giménez, B., Fernández-Martín, F., López-Caballero, M.E., Montero, M. P., Gómez-Guillén, M.C., 2012. Role of lignosulphonate in properties of fish gelatin films. Food Hydrocolloids 27 (1), 60–71.

Paarakh, M.P., Jose, P.A., Setty, C.M., Christoper, G.P., 2018. Release kinetics–concepts and applications. Int. J. Pharm. Res. Technol 8 (1), 12–20.

Pant, A.F., Özkasikci, D., Fürtauer, S., Reinelt, M., 2019. The effect of deprotonation on the reaction kinetics of an oxygen scavenger based on gallic acid. Front. Chem. 680.

Pant, A.F., Sängerlaub, S., Müller, K., 2017. Gallic acid as an oxygen scavenger in bio-based multilayer packaging films. Materials 10 (5), 489.

Parveen, S., Chaudhury, P., Dasmahapatra, U., Dasgupta, S., 2019. Biodegradable protein films from gallic acid and the cataractous eye protein isolate. Int. J. Biol. Macromol. 139, 12–20.

Picchio, M.L., Linck, Y.G., Monti, G.A., Gugliotta, L.M., Minari, R.J., Igarzabal, C.I.A., 2018. Casein films crosslinked by tannic acid for food packaging applications. Food Hydrocolloids 84, 424–434.

Quilez-Molina, A.I., Heredia-Guerrero, J.A., Armirotti, A., Paul, U.C., Athanassiou, A., Bayer, I.S., 2020. Comparison of physicochemical, mechanical and antioxidant properties of polyvinyl alcohol films containing green tealeaves waste extracts and discarded balsamic vinegar. Food Packag. Shelf Life 23, 100445.

Rani, P., Yu, X., Liu, H., Li, K., He, Y., Tian, H., Kumar, R., 2021. Material, antibacterial and anticancer properties of natural polyphenols incorporated soy protein isolate: a review. Eur. Polym. J. 152, 110494.

Requena, R., Vargas, M., Chiralt, A., 2017. Release kinetics of carvacrol and eugenol from poly (hydroxybutyrate-co-hydroxyvalerate) (PHBV) films for food packaging applications. Eur. Polym. J. 92, 185–193.

Rubilar, J.F., Cruz, R.M., Zuñiga, R.N., Khmelinskii, I., Vieira, M.C., 2017. Mathematical modeling of gallic acid release from chitosan films with grape seed extract and carvacrol. Int. J. Biol. Macromol. 104, 197–203.

Rui, L., Xie, M., Hu, B., Zhou, L., Yin, D., Zeng, X., 2017. A comparative study on chitosan/gelatin composite films with conjugated or incorporated gallic acid. Carbohydr. Polym. 173, 473–481.

Sun, X., Wang, Z., Kadouh, H., Zhou, K., 2014. The antimicrobial, mechanical, physical and structural properties of chitosan–gallic acid films. LWT–Food Sci. Technol. 57 (1), 83–89.

Sun, Y., Zhou, L., Liao, T., Liu, J., Yu, K., Zou, L., et al., 2021. Comparing the effect of benzoic acid and cinnamic acid hydroxyl derivatives on polyphenol oxidase: activity, action mechanism, and molecular docking. J. Sci. Food Agric. https://doi.org/10.1002/jsfa.11725.

Suppakul, P., Miltz, J., Sonneveld, K., Bigger, S.W., 2003. Active packaging technologies with an emphasis on antimicrobial packaging and its applications. J. Food Sci. 68 (2), 408–420.

Tapia-Hernández, J.A., Del-Toro-Sánchez, C.L., Cinco-Moroyoqui, F.J., Ruiz-Cruz, S., Juárez, J., Castro-Enríquez, D.D., et al., 2019. Gallic acid-loaded zein nanoparticles by electrospraying process. J. Food Sci. 84 (4), 818–831.

Volpe, S., Cavella, S., Masi, P., Torrieri, E., 2017. Effect of solid concentration on structure and properties of chitosan-caseinate blend films. Food Packag. Shelf Life 13, 76–84.

Xie, M., Hu, B., Wang, Y., Zeng, X., 2014. Grafting of gallic acid onto chitosan enhances antioxidant activities and alters rheological properties of the copolymer. J. Agric. Food Chem. 62 (37), 9128–9136.

Yadav, S., Mehrotra, G.K., Dutta, P.K., 2021. Chitosan based ZnO nanoparticles loaded gallic-acid films for active food packaging. Food Chem. 334, 127605.

Yong, H., Wang, X., Bai, R., Miao, Z., Zhang, X., Liu, J., 2019. Development of antioxidant and intelligent pH-sensing packaging films by incorporating purple-fleshed sweet potato extract into chitosan matrix. Food Hydrocolloids 90, 216–224.

Zarandona, I., Puertas, A.I., Dueñas, M.T., Guerrero, P., de la Caba, K., 2020. Assessment of active chitosan films incorporated with gallic acid. Food Hydrocolloids 101, 105486.

Zhao, Y., Saldaña, M.D., 2019. Use of potato by-products and gallic acid for development of bioactive film packaging by subcritical water technology. J. Supercrit. Fluids 143, 97–106.

Zhou, L., Liu, W., Xiong, Z., Zou, L., Chen, J., Liu, J., Zhong, J., 2016. Different modes of inhibition for organic acids on polyphenoloxidase. Food Chem. 199, 439–446.